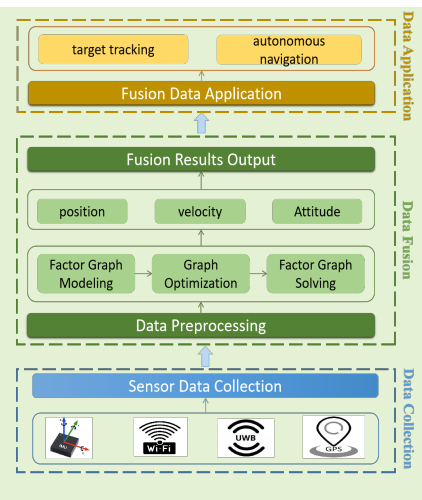


# Cooperative Localization and Mapping based on UWB/IMU Fusion using Factor Graphs

Ran Wang, *Graduate Student Member, IEEE*, Cheng Xu, *Member, IEEE*, Ruixue Li, Shihong Duan, *Member, IEEE*, and Xiaotong Zhang, *Senior Member, IEEE*

**Abstract**—In complex and unknown environments, achieving precise localization and real-time mapping stands as a critical requirement for agent navigation and scene comprehension. However, conventional localization methods, which rely on single sensors such as Inertial Measurement Units (IMUs) or Ultra-wideband (UWB) sensors, often face challenges in maintaining high precision within these intricate settings. Consequently, the task of achieving accurate self-localization and constructing topological maps becomes increasingly daunting. To tackle this challenge, we introduce a collaborative localization and mapping approach that harnesses data from both IMU and UWB sensors. We employ factor graphs as the representation model, treating observations, states, and constraints as factors within the graph. The IMU provides vital attitude and acceleration information, while the UWB sensor contributes valuable distance observations. Through the maximization of posterior probability, we estimate the agent's position and create the map. Our comprehensive evaluations conducted in physical environments conclusively demonstrate the effectiveness of our method in achieving accurate localization and mapping.

**Index Terms**—factor graph; multi-source heterogeneity; data fusion; localization; multi-target collaboration.



## I. INTRODUCTION

Simultaneous Localization and Mapping (SLAM) is a vital technology used in various fields like search and rescue, enabling robots to explore unknown underground and indoor environments [1]. The primary objective of SLAM is to estimate the agent's pose and motion over time, including its position, and construct a map of the surrounding environment using measurements from one or multiple sensors. However, achieving robust accuracy, especially in challenging indoor environments with adverse multipath channel conditions, remains a challenge [2]. These conditions often lead to perceptual degradation due to geometric reflections and obstructions, resulting in accumulated drift in position estimation. To tackle this, current systems supporting multipath channels either employ sensor technologies that mitigate multipath effects or fuse multiple sources of information [3], [4].

Multisensor data fusion is a crucial research area, especially in applications involving multi-target coordination and swarm intelligence-based localization. However, fusing multimodal

heterogeneous data presents challenges. It involves combining information from multiple sensors and processing it according to specific rules to make corresponding judgments or decisions. For example, an IMU/GPS integrated navigation system can achieve centimeter-level positioning accuracy in vehicle navigation but may not provide smooth positioning services in densely built city centers. On the other hand, the IMU/TOA fusion method combines independent measurements of IMU and the instantaneous high accuracy of TOA, offering a reliable solution for long-term and large-span positioning requirements, though it requires the deployment of fixed base stations for transmitting signals in advance, which can be expensive [5], [6].

In the context of multi-agent systems, there is a growing interest in achieving coordination and collaborative operations of heterogeneous systems in uncertain environments. For instance, a group of aerial and ground vehicles may possess different sensing, computing, and communication capabilities, or they may have different models and target sets. Therefore, sharing information in a scalable and modular manner becomes a key issue. When the underlying task requires heterogeneous robotic teams to perform local inference of certain quantities (states) of the system or environment, the problem then transforms into a data fusion problem. This research primarily focuses on data fusion algorithms, constructing a multi-sensor information fusion model, and deriving factor graph representations and nonlinear least squares formulations of probabilistic models. By adopting the approach of

This work is supported in part by the National Natural Science Foundation of China (62101029), and in part by the China Scholarship Council Award (202006465043). (*Corresponding author*: Cheng Xu)

The authors are with School of Computer and Communication Engineering, Shunde Innovation School, University of Science and Technology Beijing. Cheng Xu is also with the Institut de Recherches Interdisciplinaires et de Développements en Intelligence Artificielle (IRIDIA), Université Libre de Bruxelles, Brussels, Belgium. (email: wangran423@foxmail.com; xucheng@ustb.edu.cn; liruixue\_hebut@163.com; duansh@ustb.edu.cn; zxt@ies.ustb.edu.cn).

local/joint factors, we address the challenges faced by multi-source heterogeneous data fusion in achieving collaborative localization in multi-agent systems.

The main contributions of this study are as follows:

- 1) *Factor Graph-Based Heterogeneous Data Fusion Method*: We propose a factor graph representation for the collaborative SLAM problem, defining the problem using general terminology to describe graph operations. We show that messages between agents can be treated as factors and added to the local views of receiving agents, allowing us to fuse asynchronous information accurately, thereby improving data fusion accuracy and efficiency.
- 2) *Factor Graph-Based Belief Propagation*: We present a Bayesian detection and estimation algorithm based on Belief Propagation (BP) for estimating the state of mobile agents and the locations of beacons. Our algorithm simultaneously performs probabilistic data fusion and sequential estimation of the agent's state. BP operates on the factor graph representing the SLAM problem, leveraging conditional statistical independence for low complexity and high scalability.
- 3) *Method Validation*: We evaluate the proposed algorithm's performance using synthetic and real-world data. Experimental results demonstrate the algorithm's high accuracy and robustness compared with state-of-the-arts.

The subsequent content of this paper is organized as follows: Section II discusses related research and Section III defines the problem. Section IV describes the system framework for cooperative localization and mapping based on factor graph. Section V presents the construction process of the factor graph algorithm. Section VI provides simulation and physical experimental results. Finally, Section VII concludes the paper.

## II. RELATED WORK

### A. Filtering-based Data Fusion

In recent years, multi-sensor information fusion technology has gained significant attention in navigation research [1]. Traditional inertial navigation systems can only provide accurate results for a short time, and accumulated errors may reduce navigation accuracy, requiring auxiliary observations for bias correction. The widely used method is the Extended Kalman Filter (EKF) algorithm [7], known for its real-time computational efficiency. However, when dealing with high-dimensional state variables, integrating measurements from sensors can lead to higher computational costs, impacting real-time performance. To address the challenges of navigation accuracy and computational cost, Xu et al. [8] proposed a joint Extended Finite Impulse Response (EFIR) filter that fuses information from multiple sensors, improving navigation accuracy. Yet, in practical applications, integrated navigation systems usually use sensors with different update rates, requiring time alignment before information fusion [9], which adds complexity to the fusion process. In multi-sensor integrated navigation systems, situations where certain sensors become unavailable often occur, necessitating quick navigation system response to recover accuracy. Xiong et al. [11] proposed a robust and fault-tolerant joint filter to enhance navigation

system stability. Although joint filters are widely used due to their flexibility and fault-tolerant capabilities, their framework needs to be rebuilt when adding or removing sensors. Therefore, there is a need for research on real-time adaptive fusion methods in multi-sensor data fusion.

### B. Probabilistic Graph Models and Factor Graphs

Factor graphs [13] offer a flexible and efficient approach for implementing multi-sensor information fusion using graph optimization algorithms [14], [15]. In the factor graph framework, sensors are represented as separate factor nodes, and each node only needs to provide connectivity information to other nodes. This modular design allows easy integration of new sensors by simply adding a new node and connecting it to the existing nodes. This adaptability makes factor graphs suitable for various application scenarios. The Bayesian inference algorithms within factor graphs automatically update fusion results when new sensor nodes are added, enabling plug-and-play functionality. Previous work by Paskin et al. [16] addressed distributed inference in static sensor networks using message passing algorithms on a connected tree. However, this approach was limited to static variables and required constructing the tree before performing inference. Makarenko et al. [17] extended Paskin's algorithm for dynamic states in the Bayesian Distributed Data Fusion (DDF) problem, but it was limited to single common states in homogeneous problems. While some works explored Bayesian networks and information maps to identify conditional independence and track common information [18], they did not fully exploit the potential of Probabilistic Graphical Models (PGMs) for distributed data fusion [19].

### C. Optimization Methods for Ranging Beacons

Range measurements from range beacons are commonly processed using multilateration methods to determine positioning information [22], [23]. The most common approaches include Maximum Likelihood Estimation (MLE) solutions, such as least squares optimization [22] or Particle Swarm Optimization (PSO) [23]. Another promising optimization method is the Pose Graph SLAM framework, as demonstrated by Wang et al. [15] and Fang et al. [24]. These methods show that range measurements can effectively aid in localization, either through direct optimization or by integrating them into the Pose Graph SLAM. However, it's worth noting that these traditional methods have been primarily tested in indoor environments using range beacons with known positions. Therefore, challenges still exist when applying these methods in scenarios with sparsely deployed range beacons. Addressing these challenges and finding efficient solutions for such scenarios are areas of further research..

## III. PROBLEM DEFINITION

### A. State Model

In a two-dimensional scenario, the target nodes can acquire interaction information with other target nodes through internal and external sensors, enabling the estimation and

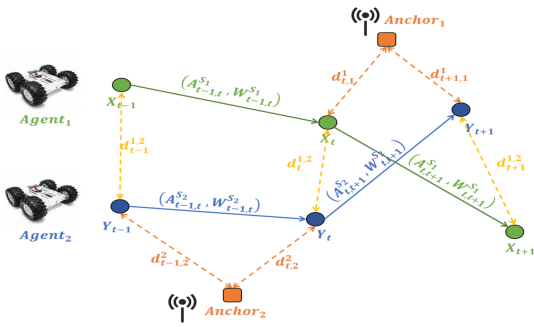


Fig. 1: The trajectory and sensing data of moving target nodes.

localization of the mobile nodes. During motion, mobile robots utilize an Inertial Measurement Unit (IMU) to control their posture, which consists of accelerometers, gyroscopes, and sometimes magnetometers [25]. However, IMUs often suffer from accumulated errors, requiring additional sensors such as UWB sensors to calibrate the biases and make more accurate predictions. Fig. 1 presents the random walk model [26] for the target nodes, where the linear acceleration  $A^S$  and angular velocity  $W^S$  can be obtained from the IMU, and distance measurement  $d_t$  can be measured using UWB. The agent can estimate the velocity  $V$ , accelerometer bias  $A^b$ , gyroscope bias  $W^b$ , position coordinates  $B$ , and attitude  $q$  of the agent by acquiring the IMU's linear acceleration  $A^S$  and angular velocity  $W^S$ . The noise during motion includes velocity  $\varepsilon_V$ , attitude  $\varepsilon_q$ , angular velocity bias  $\varepsilon_{Ab}$ , and gyroscope bias  $\varepsilon_{Wb}$ . Therefore, the state vector  $x$ , control vector  $u$ , and error vector  $\varepsilon$  can be defined as:

$$x = \begin{bmatrix} V \\ A^b \\ W^b \\ B \\ q \end{bmatrix}, u = \begin{bmatrix} A^S \\ W^S \end{bmatrix}, \varepsilon = \begin{bmatrix} \varepsilon_V \\ \varepsilon_q \\ \varepsilon_{Ab} \\ \varepsilon_{Wb} \end{bmatrix} \quad (1)$$

The state transition function is defined as:

$$X_t = Q(x_t, u_t, \varepsilon_t) = \begin{bmatrix} V_{t-1} + (R_{q(t-1)}(A_t^S + A_{t-1}^b + \varepsilon_{Ab}))\Delta t + \varepsilon_V \\ A_{t-1}^b + \varepsilon_{Ab} \\ W_{t-1}^b + \varepsilon_{Wb} \\ B_{t-1} + (V_{t-1} + \varepsilon_V)\Delta t + \frac{1}{2}(R_{q(t-1)}(A_t^S + A_{t-1}^b + \varepsilon_{Ab}))(\Delta t)^2 \\ q_{t-1} + q(W_t^S + W_{t-1}^b + \varepsilon_{Wb})\Delta t + \varepsilon_q \end{bmatrix} \quad (2)$$

In addition, the random walk follows a first-order hidden Markov model. The state of the moving target  $X_t$  at time  $t$  can be obtained by transitioning from the state  $X_{t-1}$  at time  $t-1$ . The state transition equation is as follows:

$$X_{t-1} = X_t + f(X_t, X_{t-1}) \quad (3)$$

where  $f(X_t, X_{t-1})$  is used to connect with variable nodes:

$$f(X_t, X_{t-1}) = \begin{bmatrix} X_t = Q(x_t, u_t, \varepsilon_t) \\ (R_{q(t-1)}(A_t^S + A_{t-1}^b + \varepsilon_{Ab}))\Delta t + \varepsilon_V \\ \varepsilon_{Ab} \\ \varepsilon_{Wb} \\ (V_{t-1} + \varepsilon_V)\Delta t + \frac{1}{2}(R_{q(t-1)}(A_t^S + A_{t-1}^b + \varepsilon_{Ab}))(\Delta t)^2 \\ q(W_t^S + W_{t-1}^b + \varepsilon_{Wb})\Delta t + \varepsilon_q \end{bmatrix} \quad (4)$$

## B. Measurement Model

The measurement model is typically used to combine measurements with prior information to update the target's state, which is based on measurements obtained from wireless signals or sensors such as UWB and can be represented as:

$$\hat{d}_{i,j} = d_{i,j} + \omega_1 \quad (5)$$

where  $\omega_1$  is the Gaussian-distributed distance noise, and  $d_{i,j}$  represents the true distance measurement obtained by UWB between the target's position  $(x_i, y_i)$  and  $(x_j, y_j)$ , i.e.,

$$d_{i,j} = \sqrt{(x_i - x_j)^2 + (y_i - y_j)^2} \quad (6)$$

## C. Factor Graph Representation

A factor graph is an undirected bipartite graph. In the factor graph  $G = \{F, \Theta, \varepsilon\}$ , the probability densities of  $\Theta$  in the factor graph are represented as:

$$P(\Theta|Z) = \prod_{i=1}^{|F|} P(\Theta_i|Z_i) = \prod_{i=1}^{|F|} \phi_i(\Theta_i) \quad (7)$$

where the factors  $\phi_i$  can be mainly divided into local factors and joint factors. Local factors capture the information within individual entities, while joint factors capture the interaction information between different entities, as shown in Fig. 2.

## IV. INFORMATION FUSION BASED ON FACTOR GRAPH

### A. Definition of Factors

1) **Local Factors:** They are classified into prior factors and measurement factors.

- **Prior factors:** They contain all the initial states of the agents, including position, velocity, attitude, and initial errors. The prior factors are unary factors, defined as:

$$f^{prior}(x) = d(x) \quad (8)$$

Generally, for Gaussian distributions, the prior factor can be represented using mean  $\mu_x$  and covariance  $\Sigma_x$ , namely

$$f^{prior}(x) = d(x_i) = \exp\left(-\frac{1}{2}\|x - \mu_x\|_{\Sigma_x}^2\right) \quad (9)$$

The prior factors are usually added at the initialization and play a crucial role in the solving process.

- **Measurement factors:** They are established based on the measurements obtained by the agent itself or external sensors and generally interact with other nodes, e.g., the initial position, acceleration, angle information, etc. The measurement factor for a state can be defined as:

$$f^{measure}(\ast) = d(Z^{measure} - h^{measure}(\ast)) \quad (10)$$

where  $Z^{measure}$  is the measurement value, and  $h^{measure}(\ast)$  represents the observation function. Common measurement factors include odometry factors, UWB factors, etc. Moreover:

$$Z^{measure} = h^{measure}(\ast) + n^{measure} \quad (11)$$

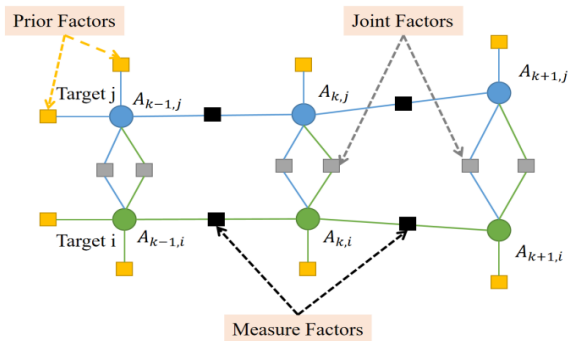


Fig. 2: The classification of factor graphs: In multi-agent cooperative localization scenarios, yellow squares represent prior factors, black squares represent measurement factors, and gray squares represent joint factors.

where  $n^{measure}$  is the measurement noise.

2) **Joint Factors:** Joint factors play a crucial role in capturing and facilitating information exchange between various entities, including range measurements among multiple agents. This real-time message passing occurs as agents move and interact with each other. For instance, in a multi-agent collaborative localization process, one agent's localization estimate for another agent can be represented as an observation factor, with the measurement value denoted as:

$$z_i^{joint}(x_i) = h^{joint}(x_i) + n^{joint} \quad (12)$$

where  $z_i^{joint}$  represents the localization information obtained at the current time,  $h^{joint}(\ast)$  represents the observation function, and  $n^{joint}$  represents the noise. In the factor graph, this observation factor can be represented as:

$$f^{joint}(x_i) = d(z_i^{joint} - h^{joint}(x_i)) \quad (13)$$

### B. Dynamic Construction

In the multi-agent collaborative localization process, the state includes various factors such as the agent's attitude, the positions of external landmarks, estimated positions of other agents, and auxiliary variables like sensor biases and sensor calibration. At time  $t_i$ , the state of an individual agent (including position, velocity, attitude, etc.) is denoted as  $x_i$ . Sensor information, estimates of other agent positions, and other external data are represented as measurements of the agent at a specific time. Let  $Z_k = z_{i=1}^k$  represent all the collected measurements from time  $t_1$  to  $t_k$ , and  $X_k = x_{i=1}^k$  represent the states. The joint probability density is expressed as  $P(X_k|Z_k)$ . The state estimation involves finding the maximum posterior probability of the state given the observations:

$$X_k^* = \underset{X_k}{\operatorname{argmax}} P(X_k|Z_k) \quad (14)$$

The algorithm flow for dynamically constructing the factor graph for multi-agent collaborative fusion localization is presented in Algorithm 1. In this algorithm,  $X_{k,1:N}$  represents the state set of  $N$  agents at time  $k$ . Moreover,

### Algorithm 1 Factor Graph-Based Multi-Sensor Fusion

**Input:**  $A_k = [X_{k,1:N}] \leftarrow$  The prior information of the initial state;  $P(X/Z) = 1 \leftarrow$  Joint probability density

**Output:**  $X_{k,1:N}^* \leftarrow$  The posterior position information of all states

```

1: for  $k \leftarrow 0, 1, 2, \dots, K$  do
2:   for (  $don \leftarrow 0, 1, 2, \dots, N$  )
3:     if  $Z_{k,n}^{prior}$  then
4:        $P(X_{k,n}/Z_{k,n}^{prior}) = f^{prior}(X_k, n)$ 
5:     end if
6:     if  $Z_{k,n}^{measurement}$  then
7:        $P(X_{k,n}/Z_{k,n}^{measurement}) = f^{measurement}(X_k, n)$ 
8:     end if
9:     if  $Z_{k,n}^{observed}$  then
10:       $P(X_{k,n}/Z_{k,n}^{observed}) = f^{observed}(X_k, n)$ 
11:    end if
12:    if  $Z_{k,n}^{joint}$  then
13:       $P(X_{k,n}/Z_{k,n}^{joint}) = f^{joint}(X_k, n)$ 
14:    end if
15:  end for
16:   $X_k^* = \underset{X_{k,1:N}}{\operatorname{argmax}} P(X_{k,n}|Z_{k,n})$ 
17: end for

```

$Z_{k,n}^{prior}$ ,  $Z_{k,n}^{measurement}$ ,  $Z_{k,n}^{observed}$ , and  $Z_{k,n}^{joint}$  represent the measurement values of the prior factor, measurement factor, observation factor, and joint factor, respectively, for the  $n$ th agent at time  $k$ .

### C. Optimization and Solving

In the factor graph  $G = \{F, \Theta, \varepsilon\}$ , the factorization can be obtained as follows:

$$f(\Theta) = \prod_i f_i(\Theta_i) \quad (15)$$

The set of variables adjacent to factor  $f_i$  is denoted by  $\Theta_i$ , where each  $f_i$  is a function of the variables in  $\Theta_i$ . The main objective is to find the optimal set  $\Theta^*$  that satisfies:

$$\Theta^* = \underset{\Theta}{\operatorname{argmax}} f(\Theta) \quad (16)$$

The measurement model is assumed to be a Gaussian, namely

$$f_i(\Theta_i) \propto \exp\left(-\frac{1}{2}\|\mathbf{h}_i(\Theta_i) - \mathbf{z}_i\|_{\Sigma_i}^2\right) \quad (17)$$

The expression  $\mathbf{h}_i(\Theta_i)$  represents the measurement function model, i.e., the theoretical value, and  $\mathbf{z}_i$  represents the measured value. The objective function is then transformed into minimizing a nonlinear least squares problem:

$$\Theta^* = \underset{\Theta}{\operatorname{argmin}} (-\log f(\Theta)) = \underset{\Theta}{\operatorname{argmin}} \sum_i \|\mathbf{h}_i(\Theta_i) - \mathbf{z}_i\|_{\Sigma_i}^2 \quad (18)$$

To transform the nonlinear least squares problem in Equation (18) into a linearized form, common approaches include



the Gauss-Newton iteration method [27] or the Levenberg-Marquardt algorithm [28]. These methods are used to iteratively solve the nonlinear equations and approximate the minimum value. During the iteration process of the nonlinear solver, linearization is performed around  $\Theta$ , also known as whitening, denoted as:  $\|e\|_{\Sigma}^2 \triangleq e^{\top} \Sigma^{-1} e = (\Sigma^{-1/2} e)^{\top} (\Sigma^{-1/2} e) = \|\Sigma^{-1/2} e\|_2^2$ . As a result, a new standard least squares problem is obtained:

$$\Delta^* = \arg \min_{\Delta} \sum_i \|A_i \Delta_i - b_i\|_2^2 = \arg \min_{\Delta} \|\mathbf{A} \Delta - \mathbf{b}\|_2^2 \quad (19)$$

where  $\Delta$  represents the state update,  $A \in \mathbb{R}^{m \times n}$  denotes Jacobian matrix of order  $m \times n$ , and  $b$  is the prediction error.

During the iterations, once  $\Delta$  is determined, it is added to  $\Theta$  to obtain the new estimate  $\Theta \oplus \Delta$  for the next iteration of nonlinear optimization. In most cases, simple addition is used for  $\oplus$ . However, when dealing with quaternions for 3D rotation and mapping, relevant Lie groups [29] are utilized instead. The probability distribution at  $\Delta$  is defined as:

$$P(\Delta) \propto e^{-\log f(\Delta)} = \exp\left(-\frac{1}{2} \|\mathbf{A} \Delta - \mathbf{b}\|_2^2\right) \quad (20)$$

The minimum value of  $\mathbf{A} \Delta - \mathbf{b}$  can be obtained using Cholesky [30] or QR decomposition [31].

## V. COOPERATIVE SLAM BASED ON FACTOR GRAPH

This section presents the sensor factor models, including the IMU factor, UWB factor, and joint factor based on UWB information. The goal is to fuse IMU and UWB sensor data in a factor graph to enhance positioning accuracy. Additionally, the method of IMU fusion for UWB mapping based on the factor graph is described, which enables the estimation of unknown UWB beacon positions using sensor information.

### A. Factor Modeling

1) *IMU Factor*: The IMU (Inertial Measurement Unit) is a sensor unit used to measure object acceleration and angular velocity, consisting of an accelerometer and a gyroscope. The IMU factor establishes constraints on IMU data in the factor graph, allowing fusion with other sensor data. The representation of the IMU factor is shown in Fig. 3, where the green hollow circles represent the state variable nodes, yellow hollow circles represent the error variable nodes, black solid circles represent the IMU factor nodes, and blue lines represent the edges in the factor graph. The IMU factor connects two adjacent state variable nodes.

Assuming the state of an entity at time  $t$  is denoted by  $x$ , which includes various parameters such as velocity  $V$ , accelerometer bias  $A^b$ , gyroscope bias  $W^b$ , position coordinates  $B$ , and attitude  $q$ . The IMU provides measurements of linear acceleration  $A^S$  and angular velocity  $W^S$ . The sensor error model is represented by  $\varepsilon$ . By utilizing Equation (4), we can derive the measurement information and observation function:

$$Z^{IMU} = \begin{bmatrix} A^S \\ W^S \end{bmatrix} \quad (21)$$

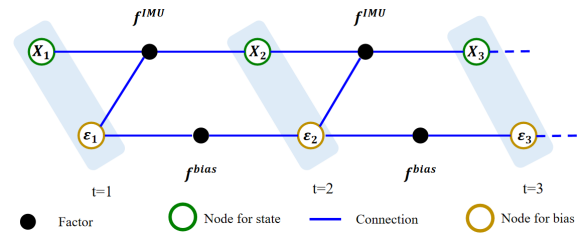


Fig. 3: IMU factor schematic diagram.

$$X = h^{IMU}(x, \varepsilon, u) = h^{IMU}(x, \varepsilon, Z^{IMU}) \quad (22)$$

By utilizing the IMU measurement information  $Z^{IMU}$ , we can establish a connection between the states  $X_k$  and  $X_{k+1}$  at two consecutive times  $t_k$  and  $t_{k+1}$ , namely

$$X_{k+1} = h^{IMU}(X_k, \varepsilon_k, z_k) \quad (23)$$

$$\varepsilon_{k+1} = g^{bias}(\varepsilon_k) \quad (24)$$

The equations above define the IMU factor node  $f^{IMU}$  to connect adjacent states  $X_k$  and  $X_{k+1}$ , and the bias factor node  $f^{bias}$  to connect adjacent variable nodes  $\varepsilon_k$  and  $\varepsilon_{k+1}$ . For Gaussian distributions, the prior factor can be represented using mean and covariance as indicated by the error functions in Equation (8) and (9), the error can be calculated as follows:

$$f^{IMU}(X_{k+1}, X_k, \varepsilon_k) = d(X_{k+1} - h^{IMU}(X_k, \varepsilon_k, z_k)) = \exp\left(-\frac{1}{2} \|X_{k+1} - h^{IMU}(X_k, \varepsilon_k, z_k)\|_{\Sigma_i}^2\right) \quad (25)$$

$$f^{bias}(\varepsilon_{k+1}) = d(\varepsilon_{k+1} - g^{bias}(\varepsilon_k)) = \exp\left(-\frac{1}{2} \|\varepsilon_{k+1} - g^{bias}(\varepsilon_k)\|_{\Sigma_i}^2\right) \quad (26)$$

Based on the analysis above, we can deduce the factor graph structure of the IMU in the factor graph-based multi-sensor information fusion localization. Fig. 3 illustrates that the IMU factor is connected to adjacent states and sensor biases. The IMU operates at a higher frequency compared to other sensors, and to address the asynchronous issue in multi-sensor fusion, IMU preintegration and variable elimination are employed, which helps reduce computation.

2) *UWB Factor*: The UWB (Ultra-Wideband) factor is another type of factor utilized for multi-sensor information fusion, specifically designed for fusing UWB measurement data. UWB factors are widely used in localization and tracking applications due to their capability of providing highly accurate distance measurements. The entity itself is equipped with UWB nodes that receive distance data from UWB beacons placed at different positions, enabling the estimation of its own position. Fig. 4 represents the UWB factor, where the green hollow circles correspond to state variable nodes, blue lines depict edges in the factor graph, black solid circles represent the IMU factors, and gray solid circles represent the UWB factors. UWB factors typically have a much lower data rate

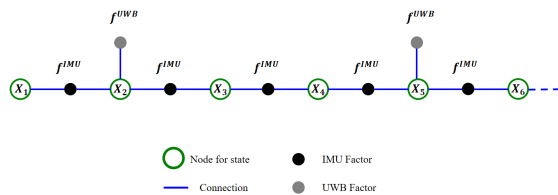


Fig. 4: UWB factor schematic diagram.

than IMU factors and are generally unary factors.

Assuming that an UWB module is installed on the agent, and there are  $n$  beacons placed on the ground, where  $n \geq 3$ . At time  $i$ , the distance measurement between the agent  $X_i$  and the  $k$ -th UWB base station  $p_k$  can be represented as  $r_{i,k}$ . Therefore, the observation function of the UWB factor can be expressed as:

$$h^{UWB}(X_i, p_k) = \|X_i - p_k\| \quad (27)$$

The UWB factor can be represented based on the relationship between the measurement value and the observation function as follows:

$$f_{UWB}(X_i, p_k, r_{i,k}) = d(r_{i,k} - h^{UWB}(X_i, p_k)) = \exp\left(-\frac{1}{2} \|r_{i,k} - h^{UWB}(X_i, p_k)\|_{\Sigma_i}^2\right) \quad (28)$$

The UWB measurement value,  $r_{i,k}$ , is solely related to the position of the entity, making the UWB factor a unary factor.

**3) Joint Factor:** In factor graph-based multi-sensor information fusion involving multiple entities, it is essential to consider the fusion and cooperation of information between entities. For this purpose, joint factors are employed to model the interaction and constraints between multiple entities. The schematic diagram of joint factors is shown in Fig. 5, where the green hollow circle represents the state variable node of the first entity, the red hollow circle represents the state variable node of the second entity, the blue lines represent the edges in the factor graph, and the black solid circles represent different factor nodes. The joint factor nodes connect two variable nodes that can receive UWB distance measurements.

When using UWB sensors for multi-entity localization, each entity can measure the distance between itself and other entities using UWB. Therefore, the distance information between each entity can be encoded as observation values, and then these joint information values can be associated with the joint state variables using distance observation functions. The joint state variables include the position and velocity information of each entity, and the joint factor combines the distance information with these state variables using the distance observation function.

Similar to the representation of the measurement value in the UWB factor, the joint information value in the joint factor represents the distance  $r_{i,j}$  between entity  $i$  and entity  $j$ , and the states of entity  $i$  and entity  $j$  are represented by  $X_i$  and  $X_j$ , respectively. The joint function is defined as:

$$h^{\text{joint}}(X_i, X_j) = \|X_i - X_j\| \quad (29)$$

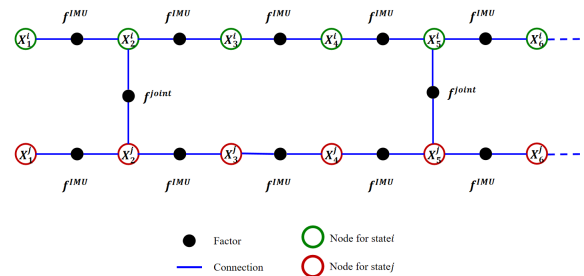


Fig. 5: The schematic diagram of joint factors.

Thus, for Gaussian distributions, the factor can be represented using mean and covariance as indicated by Equation (8) and (9), the UWB-based joint factor is obtained:

$$f_{\text{joint}}(X_i, X_j, r_{i,j}) = \exp\left(-\frac{1}{2} \|r_{i,j} - h^{\text{joint}}(X_i, X_j)\|_{\Sigma_i}^2\right) \quad (30)$$

The joint factor is related to the positions of entity  $i$  and  $j$ , making it a binary factor. The construction process is shown in Fig. 5.

### B. Localization

In the context of multi-sensor fusion localization, the goal is to estimate the position and orientation of the target using measurements from multiple sensors. This is achieved by establishing a mathematical model that combines sensor measurements with the motion model. Fig. 6 illustrates the concept of IMU fusion with UWB localization based on factor graphs. The green hollow circles and yellow hollow circles represent the state variable nodes and error variable nodes of the first entity, respectively. The red hollow circles and purple hollow circles represent the state variable nodes and error variable nodes of the second entity, respectively. The blue lines represent the edges in the factor graph, and the black solid circles represent different factor nodes. The factor nodes mainly include IMU factors, UWB factors, and UWB-based joint factors. The optimization objective function for factor graph optimization is defined as follows:

$$\arg \min_X (-\log f_{ij}(X, Z_{ij})) \quad (31)$$

where  $X$  represents the set of all unknown position and orientation variables,  $Z_{ij}$  represents the  $j$ -th measurement from the  $i$ -th sensor, and  $f_{ij}$  is a nonlinear cost function related to  $X$  and  $Z_{ij}$ .

The IMU and UWB sensors operate at different data rates, but their timestamps are aligned after data preprocessing. IMU factors connect adjacent state variables, and when UWB information is received, UWB factor nodes and joint factor nodes are introduced into the factor graph. By solving equation (31), the motion state at each time step can be obtained.

### C. Mapping

In the mapping problem, the objective is to construct a map based on sensor data, which involves estimating the

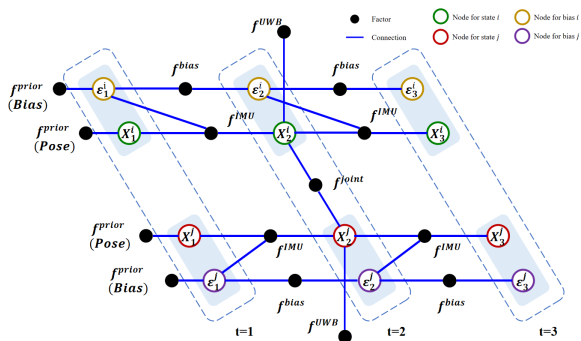


Fig. 6: Schematic diagram of IMU fusion UWB positioning based on factor graph.

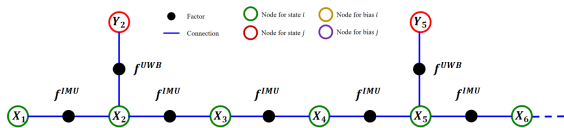


Fig. 7: Schematic diagram of IMU fusion UWB mapping based on factor graph.

positions of UWB beacons. This is achieved by representing the constraint relationship between sensor measurements and map features as factors in the factor graph. Factor graph optimization algorithms are then used to optimize these constraints and obtain the optimal map estimation.

Fig. 7 illustrates the concept of IMU fusion with UWB mapping based on factor graphs. The green hollow circles represent the state variable nodes of the entity, the red hollow circles represent the state variable nodes of the UWB ranging beacons, the blue lines represent the edges in the factor graph, and the black solid circles represent various factors. In this case, the variable set includes the estimated positions of UWB beacons. Therefore, the objective function for multi-sensor fusion mapping is defined as follows:

$$\arg \min_{(X,Y)} (-\log(f_{ij}(X, Z_{ij}) + f_k(Y_k))) \quad (32)$$

where  $X$  represents the set of all unknown position and orientation variables of the entity,  $Z_{ij}$  represents the measurement between the  $i$ -th UWB ranging beacon and the entity at time step  $j$ ,  $Y_k$  represents the position of the  $k$ -th UWB beacon,  $f_{ij}$  is a nonlinear cost function related to  $X$  and  $Z_{ij}$ , and  $f_k$  is a nonlinear cost function related to  $Y_k$ . The objective function consists of two parts: the entity's self-localization and the estimation of UWB beacon positions. By minimizing the objective function, the optimal position and orientation variables of the entity and the position variables of UWB beacons can be obtained.

The estimation of the entity's self-state follows the method described in Section V-B. In the process of estimating UWB beacon positions, the UWB factors transition from unary factors to binary factors. When the entity receives UWB ranging information at time step  $j$ , UWB factors are established, and the positions of the beacons are also estimated. Therefore, by solving equation (32), the motion state of the entity at each

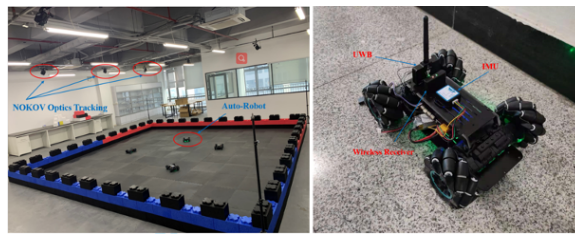


Fig. 8: (a) The scene for physical experiment. (b) The auto-robot and sensors used for the test.

time step and the positions of UWB beacons can be obtained.

## VI. EXPERIMENTS AND ANALYSIS

### A. Experimental Setup

We set up four auto-robots [32], which is equipped with UWB and IMU sensor with a sampling frequency of 200Hz and 10Hz, respectively, in a physical field (10m×10m), as shown in Fig. 8, and let them walk in random walk motion. The hardware configuration of the personal computer includes a 6-core Intel i7 CPU and 16 GB RAM, running on a 64-bit Windows 10 operating system. The sensor information and position data are collected during the experiments. The ground truth is captured by the NOKOV optics motion tracking system [33]. The IMU provides motion data for the entities, while the UWB sensors are used to estimate joint factors for multi-agent cooperative localization, sampling in 100 Hz and 10 Hz, respectively. Furthermore, the trajectory paths and localization errors are considered to evaluate the algorithm's performance.

### B. Multi-Agent Localization

The objective of this experiment is to validate the effectiveness of the algorithm by comparing the localization performance with varying numbers of entities. The experiment utilizes the simulated scenario depicted in Fig. 8, with the same four beacon positions. By introducing different numbers of entities, we compare the localization performance, and the results demonstrate that the proposed algorithm achieves reduced localization errors that stabilize as the number of entities increases.

In the specific experiment, Fig. 9 illustrates the localization errors under different numbers of entities. It shows that as the number of entities increases, the localization errors gradually decrease and stabilize after reaching a certain level. This indicates that the proposed multi-agent, multi-sensor fusion localization algorithm possesses good robustness and accuracy.

Furthermore, Fig. 10 illustrates the cooperative localization errors of four entities, which stabilize within 0.1 m. These results further demonstrate the good localization performance of the proposed algorithm under multi-agent cooperation.

Based on this experiment, we can conclude that the proposed multi-sensor fusion localization algorithm based on factor graphs exhibits excellent localization performance under multi-agent cooperation. It effectively reduces localization errors and is applicable to larger and more complex scenarios, displaying scalability. This algorithm holds significant application value for multi-agent localization in practical scenarios.

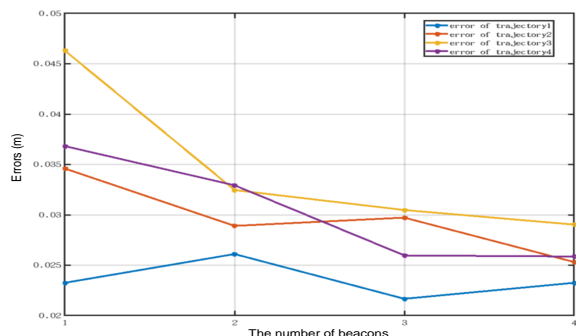


Fig. 9: Positioning error under different numbers of agents.

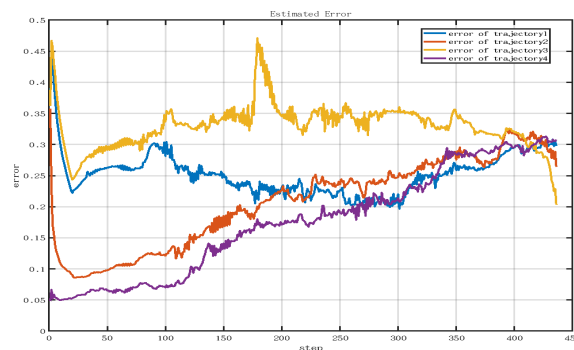


Fig. 11: The positioning error of the intelligent agent under the initial unknown condition of the ranging beacon.

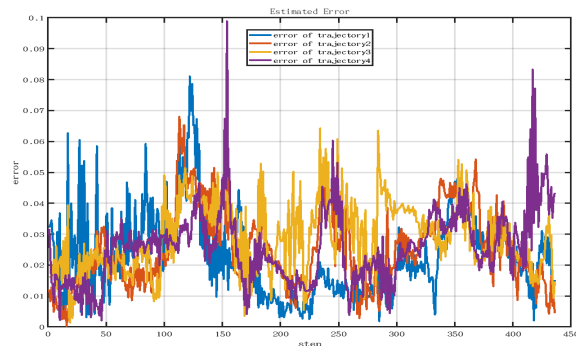


Fig. 10: Error map for collaborative positioning of four intelligent agents.

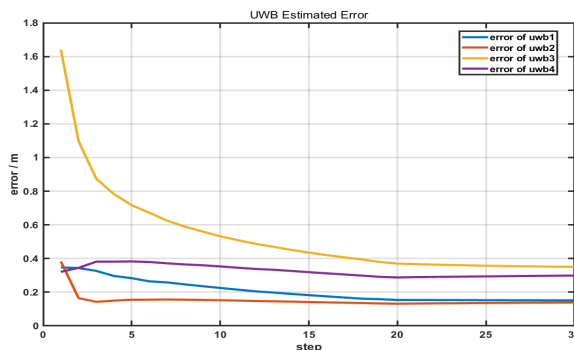


Fig. 12: UWB mapping error in the case of unknown initial range beacon.

### C. Multi-Agent Mapping

In this experiment, we employ the multi-agent fusion mapping approach using sensor information to estimate the positions of the entities and four UWB ranging beacons. The data from IMU and UWB sensors are collected in the same experimental scenario as described in Section VI-B, where four UWB ranging beacons have initially unknown positions. The entities move through random walks in the scenario, recording their own positions and the distance information to the four beacons. We use the factor graph approach for mapping and information fusion to obtain more accurate position estimation results.

Fig. 11 illustrates the localization errors of the entities when the positions of the ranging beacons are initially unknown, with errors stabilized within 0.5m for all four entities. Fig. 12 represents the mapping errors of UWB when the positions of the ranging beacons are initially unknown. By analyzing the localization error graph of the four beacons, it can be observed that the localization errors gradually decrease and stabilize within a small range. This demonstrates the effectiveness of the factor graph approach for solving the mapping problem and obtaining high-precision localization results.

In summary, this experiment validates the effectiveness of the factor graph approach for multi-agent fusion mapping, providing reasonably accurate estimation results of the positions of the entities and beacons. These results offer a solution for mapping in multi-agent systems and provide valuable data and experience for research and applications in related fields.

### D. Robustness Analysis

To validate the influence of different experimental parameters on the algorithm's performance, an analysis is conducted on parameters such as the number of target beacons and communication range.

1) *Number of Beacons*: In order to conduct a more in-depth analysis of the impact of the number of beacons on different sensor fusion algorithms, this study investigates the effect by varying the number of UWB beacons. Filed comparison tests are conducted using state-of-the-art EKF [34], and PF [35] algorithms, and the factor graph-based fusion algorithm. The experiments test the cases of simultaneously receiving different numbers of beacons and record the estimation errors of both the entities and beacons. Fig. 13 and Table I summarize the results of the experiment, showcasing the estimation errors for different algorithms under varying numbers of beacons. This analysis provides insights into the robustness of the factor graph-based fusion algorithm compared to others.

The experimental results clearly demonstrate that the factor graph-based fusion algorithm achieves superior localization accuracy, especially under different numbers of beacons. When compared to other traditional localization algorithms, the factor graph-based fusion algorithm exhibits better scalability and applicability, making it well-suited for localization tasks in large-scale scenarios. As a result, the proposed algorithm proves to have excellent scalability and offers a more reliable localization solution for practical applications.



TABLE I: Average errors (m) under different number of beacons.

| Algorithm    | Average error of 3 beacons | Average error of 4 beacons | Average error of 5 beacons | Average error of 6 beacons | Average error of 7 beacons |
|--------------|----------------------------|----------------------------|----------------------------|----------------------------|----------------------------|
| EKF [34]     | 0.572473                   | 0.407710                   | 0.451948                   | 0.386859                   | 0.471585                   |
| PF [35]      | 0.245112                   | 0.152310                   | 0.132196                   | 0.081148                   | 0.079118                   |
| Factor Graph | 0.048761                   | 0.034730                   | 0.116158                   | 0.072352                   | 0.059008                   |

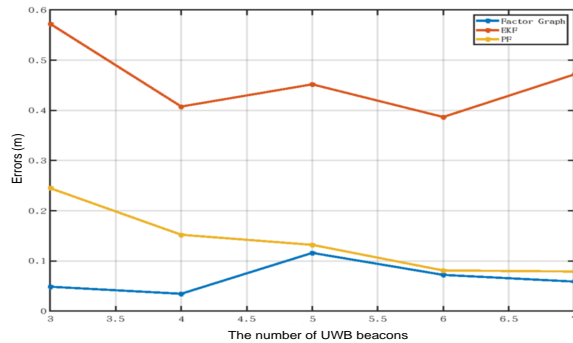


Fig. 13: Positioning error under different UWB communication ranges.

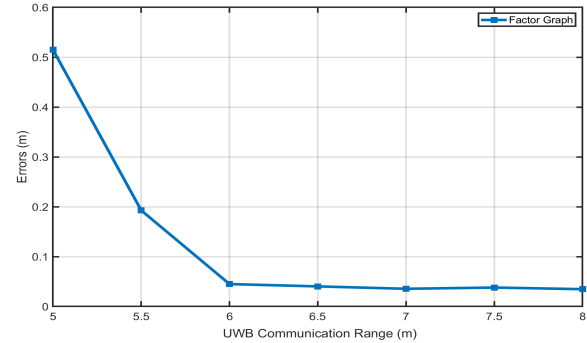


Fig. 14: Positioning error when receiving different numbers of beacons.

2) *Communication Range*: To investigate the impact of measurement thresholds on the algorithm, experiments are conducted with UWB sensors under different measurement ranges, and the position estimation errors of the entities are recorded. The experimental results, as shown in Fig. 14, indicate that larger measurement ranges lead to smaller localization errors. This is because when the UWB sensor's measurement range is smaller, the measurement errors tend to be larger. However, as the measurement range increases, the UWB sensor can collect more information, which helps reduce the errors. Nevertheless, it is crucial to strike a balance as excessively large measurement ranges introduce more interference and noise, resulting in diminishing returns in error reduction.

Therefore, in practical applications, selecting appropriate sensor communication ranges based on different scenarios and performing suitable algorithm optimizations are necessary steps to improve localization accuracy and robustness.

## VII. CONCLUSION

This paper introduces a factor graph-based algorithm for multi-sensor information fusion, which aims to address challenges related to positioning errors and map construction in sensor fusion. The proposed algorithm provides a comprehensive framework for multi-sensor information fusion, encompassing data acquisition, fusion, and application. To evaluate the algorithm's robustness, a series of experiments are conducted, analyzing the impact of parameters such as the number of beacons and communication range. The experimental results clearly demonstrate the effectiveness of the proposed algorithm under various parameter settings, effectively addressing the challenges associated with positioning errors and map construction in sensor information fusion.

## REFERENCES

- [1] C. Cadena, L. Carlone, H. Carrillo, and et al., "Past, present, and future of simultaneous localization and mapping: Toward the robust-perception age," *IEEE Transactions on Robotics*, vol. 32, no. 6, pp. 1309–1332, 2016.
- [2] T. Yang, A. Cabani, and H. Chafouk, "A survey of recent indoor localization scenarios and methodologies," *Sensors*, vol. 21, no. 23, p. 8086, 2021.
- [3] Y. Zhao, Z. Li, B. Hao, and J. Shi, "Sensor selection for tdoa-based localization in wireless sensor networks with non-line-of-sight condition," *IEEE Transactions on Vehicular Technology*, vol. 68, no. 10, pp. 9935–9950, 2019.
- [4] X. Guo, N. Ansari, F. Hu, Y. Shao, N. R. Elikplim, and L. Li, "A survey on fusion-based indoor positioning," *IEEE Communications Surveys & Tutorials*, vol. 22, no. 1, pp. 566–594, 2019.
- [5] Y. Liu, Q. Luo, and Y. Zhou, "Deep learning-enabled fusion to bridge gps outages for ins/gps integrated navigation," *IEEE Sensors Journal*, vol. 22, no. 9, pp. 8974–8985, 2022.
- [6] H. Obeidat, W. Shuaieb, O. Obeidat, and R. Abd-Alhameed, "A review of indoor localization techniques and wireless technologies," *Wireless Personal Communications*, vol. 119, pp. 289–327, 2021.
- [7] T. Bailey, J. Nieto, J. Guivant, and et al., "Consistency of the ekf-slam algorithm," in *2006 IEEE/RSJ International Conference on Intelligent Robots and Systems*. IEEE, 2006, pp. 3562–3568.
- [8] Y. Xu, G. Tian, and X. Chen, "Enhancing ins/uwb integrated position estimation using federated efr filtering," *IEEE Access*, vol. 6, pp. 64 461–64 469, 2018.
- [9] W. Li, H. Leung, and Y. Zhou, "Space-time registration of radar and esm using unscented kalman filter," *IEEE Transactions on Aerospace and Electronic Systems*, vol. 40, no. 3, pp. 824–836, 2004.
- [10] Z. Jiao, "Research on asynchronous registration method based on improved unequal-interval federated filter," in *2019 IEEE 3rd Information Technology, Networking, Electronic and Automation Control Conference (ITNEC)*. IEEE, 2019, pp. 2320–2323.
- [11] H. Xiong, R. Bian, Y. Li, and et al., "Fault-tolerant gnss/sins/dvl/cns integrated navigation and positioning mechanism based on adaptive information sharing factors," *IEEE Systems Journal*, vol. 14, no. 3, pp. 3744–3754, 2020.
- [12] W. Jiang, S. Chen, B. Cai, and et al., "A multi-sensor positioning method-based train localization system for low density line," *IEEE Transactions on Vehicular Technology*, vol. 67, no. 11, pp. 10 425–10 437, 2018.
- [13] N. Wiberg, H. A. Loeliger, and R. Kotter, "Codes and iterative decoding

- on general graphs,” *European Transactions on Telecommunications*, vol. 6, no. 5, pp. 513–525, 1995.
- [14] F. J. Perez-Grau, F. Caballero, L. Merino, and et al., “Multi-modal mapping and localization of unmanned aerial robots based on ultra-wideband and rgb-d sensing,” in *2017 IEEE/RSJ International Conference on Intelligent Robots and Systems (IROS)*. IEEE, 2017, pp. 3495–3502.
  - [15] C. Wang, H. Zhang, T. M. Nguyen, and et al., “Ultra-wideband aided fast localization and mapping system,” in *2017 IEEE/RSJ International Conference on Intelligent Robots and Systems (IROS)*. IEEE, 2017, pp. 1602–1609.
  - [16] M. Paskin and C. E. Guestrin, “Robust probabilistic inference in distributed systems,” 2004. [Online]. Available: <http://arxiv.org/abs/1207.4174>
  - [17] A. Makarenko, A. Brooks, T. Kaupp, H. Durrant-Whyte, and F. Dellaert, “Decentralised data fusion: A graphical model approach,” in *2009 12th International Conference on Information Fusion*, Jul. 2009, pp. 545–554.
  - [18] C.-Y. Chong and S. Mori, “Graphical models for nonlinear distributed estimation,” in *Proceedings of the 7th International Conference on Information Fusion (FUSION)*, 2004, pp. 614–621.
  - [19] F. Dellaert, “Factor graphs: exploiting structure in robotics,” *Annual Review of Control, Robotics, and Autonomous Systems*, vol. 4, no. 1, pp. 141–166, 2021.
  - [20] A. Cunningham, V. Indelman, and F. Dellaert, “Ddf-sam 2.0: consistent distributed smoothing and mapping,” in *2013 IEEE International Conference on Robotics and Automation (ICRA)*, 2013, pp. 5220–5227.
  - [21] B. Etzlinger, F. Meyer, F. Hlawatsch, A. Springer, and H. Wymeersch, “Cooperative simultaneous localization and synchronization in mobile agent networks,” *IEEE Transactions on Signal Processing*, vol. 65, no. 14, pp. 3587–3602, Jul. 2017.
  - [22] K.-M. Mimoune, I. Ahriz, and J. Guillory, “Evaluation and improvement of localization algorithms based on uwb pozyx system,” in *Proc. Int. Conf. Softw., Telecommun. Comput. Netw. (SoftCOM)*, 2019, pp. 1–5.
  - [23] W. Gao, G. Kamath, K. Veeramachaneni, and L. Osadciw, “A particle swarm optimization based multilateration algorithm for uwb sensor network,” in *Proc. Conf. Elect. Comput. Eng.*, 2009, pp. 950–953.
  - [24] X. Fang, C. Wang, T.-M. Nguyen, and L. Xie, “Graph optimization approach to localization with range measurements,” 2018.
  - [25] T. Ruan and R. Balch, “Rpm measurement using mems inertial measurement unit (imu),” in *Proceedings of the International Conference on Embedded Systems, Cyber-Physical Systems, and Applications (ESCS)*, 2018, pp. 49–53.
  - [26] E. A. Codling, M. J. Plank, and S. Benhamou, “Random walk models in biology,” *Journal of the Royal Society Interface*, vol. 5, no. 25, pp. 813–834, 2008.
  - [27] S. Gratton, A. S. Lawless, and N. K. Nichols, “Approximate gauss–newton methods for nonlinear least squares problems,” *SIAM Journal on Optimization*, vol. 18, no. 1, pp. 106–132, 2007.
  - [28] J. J. Moré, “The levenberg-marquardt algorithm: implementation and theory,” in *Numerical analysis: proceedings of the biennial Conference held at Dundee, June 28–July 1, 1977*. Springer, 2006, pp. 105–116.
  - [29] D. Q. Huynh, “Metrics for 3d rotations: Comparison and analysis,” *Journal of Mathematical Imaging and Vision*, vol. 35, pp. 155–164, 2009.
  - [30] N. J. Higham, “Cholesky factorization,” *Wiley interdisciplinary reviews: computational statistics*, vol. 1, no. 2, pp. 251–254, 2009.
  - [31] H. Bouwmeester, M. Jacquelin, J. Langou, and et al., “Tiled qr factorization algorithms,” in *Proceedings of 2011 International Conference for High Performance Computing, Networking, Storage and Analysis*, 2011, pp. 1–11.
  - [32] Nooploop, “Autorobo,” <https://www.nooploop.com/en/autorobo/>, accessed on 2023-07-21.
  - [33] “Nokov,” <https://en.nokov.com/direct>, accessed on 2023-07-21.
  - [34] Y. Huang, Y. Zhang, B. Xu, Z. Wu, and J. A. Chambers, “A new adaptive extended kalman filter for cooperative localization,” *IEEE Transactions on Aerospace and Electronic Systems*, vol. 54, no. 1, pp. 353–368, 2017.
  - [35] L. Wielandner, E. Leitinger, F. Meyer, and K. Witrisal, “Message passing-based 9-d cooperative localization and navigation with embedded particle flow,” *IEEE Transactions on Signal and Information Processing over Networks*, vol. 9, pp. 95–109, 2023.

from the University of Science and Technology Beijing (USTB), China in 2016. She is currently working toward the Doctoral degree at University of Science and Technology Beijing. Her research interests include quantum optimization, distributed security and internet of things.

**Cheng Xu** received the B.E., M.S. and Ph.D. degree from the University of Science and Technology Beijing(USTB), China in 2012, 2015 and 2019 respectively. He is currently working as an associate professor at University of Science and Technology Beijing. He is supported by the Post-doctoral Innovative Talent Support Program from Chinese government in 2019. He is an associate editor of International Journal of Wireless Information Networks. His research interests now include swarm intelligence and multi-robots network.

**Ruixue Li** received her Master degree from University of Science and Technology Beijing (USTB), China in 2023. Her research interests include distributed security and internet of things.

**Shihong Duan** received Ph.D. degree in computer science from University of Science and Technology Beijing (USTB), in 2012. She is an associate professor with the School of Computer and Communication Engineering, USTB . Her research interests includes wireless indoor positioning, human gesture recognition and motion capture.

**Xiaotong Zhang** received the M.S., and Ph.D. degrees from University of Science and Technology Beijing, in 1997, and 2000, respectively. He is a Professor at University of Science and Technology Beijing. His research includes work in signal processing of communication and computer architecture.

**Ran Wang** received the B.E. degree from the Beijing Information Science and Technology University, China in 2013, and the M.S. degree